J|A|C|S
ARTICLES
Published on Web 10/14/2006

Carbene vs Olefin Products of C−H Activation on Ruthenium via Competing α- and β-H Elimination

Vladimir F. Kuznetsov,[†,§] Kamaluddin Abdur-Rashid,[†,||] Alan J. Lough,[‡] and Dmitry G. Gusev*[,†]

Contribution from the Department of Chemistry, Wilfrid Laurier University, Waterloo, Ontario N2L 3C5 Canada, and Department of Chemistry, University of Toronto, Toronto, Ontario M5S 3H6, Cananda

Received July 21, 2006; E-mail: dgoussev@wlu.ca

Abstract: Bulky pincer complexes of ruthenium are capable of C−H activation and H-elimination from the pincer ligand backbone to produce mixtures of olefin and carbene products. To characterize the products and determine the mechanisms of the C−H cleavage, reactions of $[RuCl_2(p\text{-cymene})]_2$ with *N,N′*-bis(di-*tert*-butylphosphino)-1,3-diaminopropane (**L1**) and 1,3-bis(di-*tert*-butylphosphinomethyl)cyclohexane (**L2**) were studied using a combination of X-ray crystallography, NMR spectroscopy, and DFT computational techniques. The reaction of **L1** afforded a mixture of an alkylidene, a Fischer carbene, and two olefin isomers of the 16-e monohydride $RuHCl[^tBu_2PNHC_3H_4NHPBu^t_2]$ (**2**), whereas the reaction of **L2** gave two olefin and two alkylidene isomers of 16-e $RuHCl[2,6\text{-}(CH_2PBu^t_2)_2C_6H_8]$ (**3**), all resulting from dehydrogenations of the ligand backbone of **L1** and **L2**. The key intermediates implicated in the C−H activation reactions were identified as 14-electron paramagnetic species RuCl(PCP), where PCP = cyclometalated **L1** or **L2**. Thus the α- and β-H elimination reactions of RuCl(PCP) involved spin change and were formally spin-forbidden. Hydrogenation of **2** and **3** afforded 16-electron dihydrides $RuH_2Cl(PCP)$ distinguished by a large quantum exchange coupling between the hydrides.

Introduction

Transition metal alkyls possessing β-hydrogens can be unstable with respect to β-H elimination, a central reaction of organometallic chemistry.[1] Two features are important for facile β-elimination as shown in Scheme 1: (i) an empty coordination site on the metal and (ii) a syn coplanar (or nearly coplanar) arrangement of the $M-C_\alpha-C_\beta-H$ atoms. Metal alkyls in which the metal, the C−C bond, and a β-hydrogen cannot become coplanar either do not undergo elimination or do so at a very slow rate. Examples of stable systems possessing β-hydrogens include cyclic dialkyls where the β-C−H bonds are directed away from the metal and are not available for elimination.[1b] Although β-hydrogen elimination was invoked to rationalize some transformations of metalacyclobutane and -pentane complexes,[2] examples of the reaction in Scheme 1 are not known for cyclic dialkyls.

Scheme 1

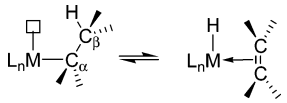

A facile β-H elimination and olefin insertion process has been detected by us in the five-atom metalacycles of RuHCl(Py)-$[^tBu_2PCH_2CH_2((E)\text{-}CH{=}CH)CH_2PBu^t_2]$.[3] The sequence of reactions shown in Scheme 2 was observed as an exchange process on the ^1H NMR relaxation time scale that allowed the determination of the barrier for this rearrangement, $\Delta G^‡ = 18.5$ kcal/mol. A transition structure for β-H elimination from the five-coordinate 16-electron intermediate in Scheme 2 was optimized in a DFT calculation, which predicted a small $Ru-C_\alpha-C_\beta-H$ dihedral angle of 23°. This demonstrates that cyclometalated transition metal complexes are not as rigid as they may appear and, in some cases, can relatively easily undergo β-H elimination. β-H elimination must have played a role in the formation

[†] Wilfrid Laurier University.
[‡] University of Toronto.
[§] Present address: Cody Laboratories, 601 Yellowstone Avenue, Cody, WY 82414.
[||] Present address: Kanata Chemical Technologies, 310-101 College Street, MaRS Centre, Toronto, Ontario M5G 12L7, Canada.

(1) (a) Collman, J. P.; Hegedus, L. S.; Norton, J. R.; Finke, R. G. *Principles and Applications of Organotransition Metal Chemistry*; University Science Books: Mill Valley, CA, 1987. (b) Crabtree, R. H. *The Organometallic Chemistry of the Transition Metals*, 3rd ed.; Wiley: New York, 2001. These reactions have been extensively studied by theoretical methods: (c) Niu, S.; Hall, M. B. *Chem. Rev.* **2000**, *100*, 353. (d) Koga, N.; Morokuma, K. *Transition Metal Hydrides*; Dedieu, A., Ed.; VCH: New York, 1992; p 185.

(2) (a) Slugovc, C.; Mereiter, K.; Schmid, R.; Kirchner, K. *Eur. J. Inorg. Chem.* **1999**, *7*, 1141. (b) Lindner, E.; Wassing, W. *Organometallics* **1991**, *10*, 1640. (c) Yang, G. K.; Bergman, R. G. *Organometallics* **1985**, *4*, 129. (d) Yang, G. K.; Bergman, R. G. *J. Am. Chem. Soc.* **1983**, *105*, 6500. (e) McLain, S. J.; Sancho, J.; Schrock, R. R. *J. Am. Chem. Soc.* **1979**, *101*, 5451. (e) Grubbs, R. H.; Miyashita, A.; Liu, M.; Burk, P. *J. Am. Chem. Soc.* **1977**, *99*, 3863. (f) Grubbs, R. H.; Miyashita, A.; Liu, M.; Burk, P. *J. Am. Chem. Soc.* **1978**, *100*, 2418. (g) Grubbs, R. H.; Miyashita, A. *J. Am. Chem. Soc.* **1978**, *100*, 1300. (h) Grubbs, R. H.; Miyashita, A. *J. Am. Chem. Soc.* **1978**, *100*, 7416. (i) Grubbs, R. H.; Miyashita, A. *J. Am. Chem. Soc.* **1978**, *100*, 7418. (j) McKinney, R. J.; Thorn, D. L.; Hoffmann, R.; Stockis, A. *J. Am. Chem. Soc.* **1981**, *103*, 2595.

(3) Gusev, D. G.; Lough, A. J. *Organometallics* **2002**, *21*, 5091.

10.1021/ja065249g CCC: $33.50

Scheme 2 [a]

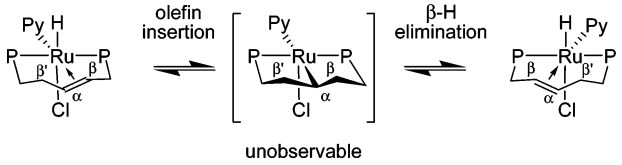

[a] P = PBu^t_2.

Chart 1. [a]

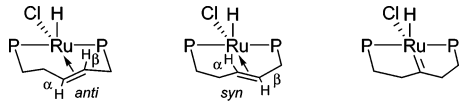

[a] P = PBu^t_2.

Scheme 3

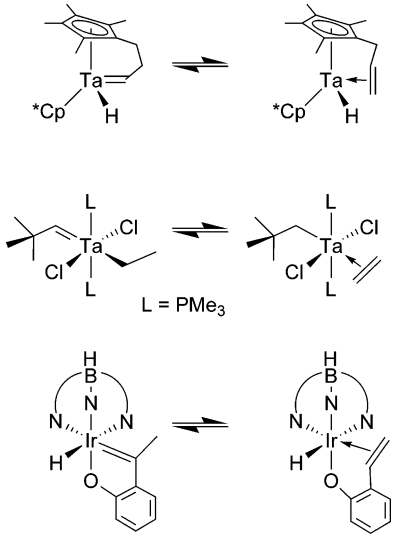

of another olefin complex of ruthenium, RuHCl[^{t}Bu$_2$PCH$_2$-CH$_2$((*E*)-CH═CH)CH$_2$PBu^t_2] (**1**), which was obtained by dehydrogenation of 1,5-bis(di-*tert*-butylphosphino)pentane (D^{t}BPP) in a reaction with [RuCl$_2$(*p*-cymene)]$_2$.[4] The product compound was isolated as a mixture of isomers **1a** and **1b** distinguished by the syn and anti configurations of their HC$_\alpha$–RuH fragments according to Chart 1. The product mixture also contained a small amount of a species which was tentatively assigned as carbene structure **1c**. This suggested that α-H elimination could compete with *β*-H elimination to produce an equilibrium mixture of alkylidene and olefin isomers. A precedent for isomeric alkylidene and alkene structures is limited to the examples[5] shown in Scheme 3, and this type of rearrangement has received limited attention,[5e] despite being highly relevant to activation of C–H bonds, olefin metathesis, and functionalization of hydrocarbons.

We thus decided to synthesize ruthenium compounds with analogues of D^{t}BPP such as bulky diphosphines **L1** and **L2**,

(4) Gusev, D. G.; Lough A. J. *Organometallics* **2002**, *21*, 2601.
(5) (a) Fellman, J. D.; Schrock, R. R.; Traficante, D. D. *Organometallics* **1982**, *1*, 481. (b) Parkin, G.; Bunel, E.; Burger, B. J.; Trimmer, M. S.; van Asselt, A.; Bercaw, J. E. *J. Mol. Catal.* **1987**, *41*, 21. (c) Paneque, M.; Poveda, M. L.; Santos, L. L.; Carmona, E.; Lledós, A.; Ujaque, G.; Mereiter, K. *Angew. Chem., Int. Ed.* **2004**, *43*, 3708. (d) For a discussion of α- vs *β*-hydrogen elimination reactions producing isomeric Fischer carbene vs alkene complexes, see: Carmona, E.; Paneque, M.; Poveda, M. *Dalton Trans.* **2003**, 4022. (e) Olefin to alkylidene rearrangements on early transition metals, Nb and Ta, were recently discussed by: Hirsekorn, K. F.; Veige, A. S.; Marchak, M. P.; Koldobskaya, Y.; Wolczanski, P. T.; Cundari, T. R.; Lobkovsky, E. B. *J. Am. Chem. Soc.* **2005**, *127*, 4809.

Chart 2

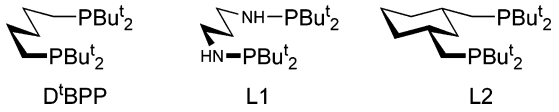

shown in Chart 2, and investigate the effect of the structural modifications on the dehydrogenation of the ligands and structural preferences of the metal products. This strategy proved productive and resulted in the isolation of a series of novel olefin and carbene complexes of ruthenium. In this paper, we report the structure and detailed isomerization mechanisms of the new compounds established by a combination of experimental and computational methods. This paper also reports hydrogenation reactions of the unsaturated complexes that have afforded new Ru(IV) dihydride products exhibiting quantum exchange couplings in ^{1}H NMR spectra.

Results and Discussion

Part 1, Reaction of L1. Heating a toluene solution of [RuCl$_2$-(*p*-cymene)]$_2$ with *N*,*N*′-bis(di-*tert*-butylphosphino)-1,3-diaminopropane (**L1**) in the presence of 1 equiv of triethylamine resulted in dehydrogenation of **L1** and formation of the monohydride RuHCl[^{t}Bu$_2$PNHC$_3$H$_4$NHPBu^t_2] (**2**) as a mixture of four isomers **2a**–**d**, according to the reaction equation:

$$^1/_2[RuCl_2(p\text{-cymene})]_2 + \mathbf{L1} + Et_3N \rightarrow \mathbf{2} + Et_3N{\cdot}HCl + p\text{-cymene}$$

Chart 3. [a]

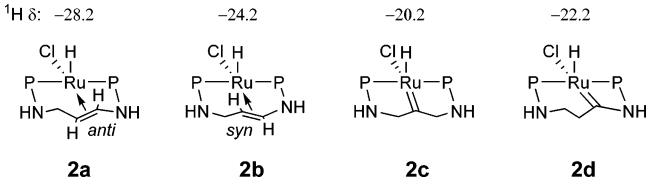

[a] P = PBu^t_2.

The isolated product contained isomer **2a** as the major species (>90%) which could be obtained in pure form by recrystallization. Different relative amounts of the other isomers were observed in solutions of **2** depending on time and temperature. The equilibrium between **2a** and **2c** was established sufficiently rapidly to be observed at room temperature. In contrast, formation of **2b** and **2d** from **2a** was slow and did not proceed at room temperature in THF-d_8. An equilibrium was established after 3 d of heating the THF solution at 75 °C, and the following composition was determined by integration of the hydride resonances: **2a** (62.7%, 0 kcal/mol), **2b** (13.6%, ΔG = 1.1 kcal/mol), **2c** (8.4%, ΔG = 1.4 kcal/mol), and **2d** (15.3%, ΔG = 1.0 kcal/mol). The ratio did not change upon further heating for 4 d, and there was no observable degradation of the sample.

Formation of **2c** from pure **2a** was monitored by ^{1}H NMR spectroscopy at 20 °C. The concentration of **2c** increased in a linear fashion in the first 2 h allowing the determination of the rate constant $k = 2.7 \times 10^{-6}$ s^{-1} and the activation energy $\Delta G^{\ddagger}$ = 24.6 kcal/mol for the isomerization of **2a** into **2c**. Interestingly, either crystalline **2a** did not undergo isomerization or the equilibrium amount of **2c** was very small in the solid state. Even after several weeks of storing crystalline **2a** at room temperature,

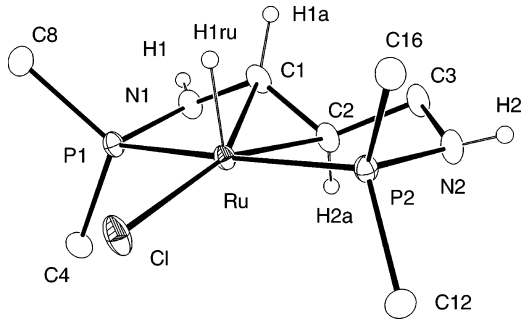

Figure 1. Crystal structure of **2a**. For clarity, hydrogen atoms bonded to C3 and all CH_3 groups have been omitted, and only one molecule (A) in the asymmetric unit is shown. Thermal ellipsoids are drawn at 30% probability. Selected bond distances [Å] and angles [deg]: Ru−Hru 1.47(3), Ru−C1 2.172(2), Ru−C2 2.157(2), Ru−P1 2.3568(6), Ru−P2 2.3390(6), Ru−Cl 2.4019(6), C1−C2 1.398(4), N1−C1 1.454(3), N2−C3 1.458(3), C2−Ru−Hru 103(1), Hru−Ru−Cl 93.4(10), P1−Ru−P2 171.24(2), C2−Ru−Cl 161.67(7), C1−C2−Ru−Hru 53.6.

the NMR spectrum of a freshly prepared solution showed only a trace amount of **2c**.

The structure of **2a** was determined by X-ray diffraction. It is shown in Figure 1 and is very similar to the corresponding structure of RuHCl[^{t}Bu$_2$PCH$_2$CH$_2$((*E*)-CH═CH)CH$_2$PBu$^t_2$] (isomer **1a** in Chart 1). The structural assignment of **2b** according to Chart 3 was based on the hydride ^{1}H NMR shift and $^2J_{H-P}$ coupling closely matching the spectral characteristics of the corresponding isomer **1b**. The coordinated olefin fragment of **2b** was observed at δ 60.9 and 70.9 in the ^{13}C{^{1}H} NMR spectrum. For **2c**, using a concentrated solution of **2** in CD_2Cl_2, we were able to acquire a ^{13}C{^{1}H} NMR spectrum that showed the carbene resonance as a triplet at 318 ppm. Other key NMR data for **2c**, such as the observation of a single ^{31}P peak and a triplet hydride resonance, confirmed the formulation of the complex as a C_s symmetric carbene RuHCl[═C(CH$_2$NHPBu$^t_2$)$_2$].

Isomer **2d** had no structural analogue in the system of **1**. It was distinguished from the other isomers of **2** by reduced solubility (<5 mg/mL) in common solvents such as toluene, THF, or dichloromethane. After heating a toluene solution of **2** for 24 h at 90 °C, we obtained a precipitate containing 88% of **2d** cocrystallized with small amounts of **2a**−**c**. The isolated solid was well soluble in *N*-methylpyrrolidinone (NMP) that allowed the acquisition of ^{13}C{^{1}H} NMR and ^{13}C DEPT spectra. The observation of a quaternary carbon resonance at 275 ppm and two CH_2 resonances at 44.8 and 46.5 ppm suggested the structural interpretation of **2d** as a Fischer carbene complex. The trans arrangement of the phosphorus atoms in **2d** was confirmed by the observation of a large $^2J_{P-P}$ coupling of 300 Hz in the ^{31}P{^{1}H} NMR spectrum. Two important pieces of structural information were obtained from the proton spectra of **2d** in CD_2Cl_2: (i) an NOE was detected between the hydride and only one (H_a) of the four hydrogens of the ligand backbone, and (ii) hydrogen H_b (bonded to the same carbon as H_a) showed equal couplings to H_c and H_d of the neighboring methylene group, which suggested that the dihedral angles $H_b-C-C-H_c$ and $H_b-C-C-H_d$ could be very similar. These conditions are satisfied in the representation of **2d** diagrammed in Chart 4. The ^{1}H NMR spectra of **2d** showed nonequivalent NH proton chemical shifts at δ 2.0 and 7.8 in CD_2Cl_2. The distinct low-field shift could be due to the hydrogen of the partial double C−NH bond.

Minor isomers of **2** could not be characterized by X-ray crystallography. Therefore, we optimized geometries of all four

Chart 4

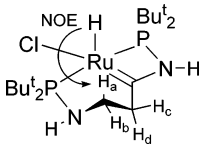

species **2a**-**d** in a series of DFT calculations. The calculated structures are shown in Figure 2 and a list of selected bond distances and angles is given in the figure's caption. Isomer **2a** was optimized first and when the crystal structure became available, a comparison of the calculated and experimental geometries revealed excellent agreement for the principal bond distances and angles, with the differences not exceeding 0.016 Å and 1.8°, respectively. The calculated geometry of **2b** is also very similar to the crystal structure of **1b**. We assume that the calculated structures of **2b**, **2c**, and **2d** in Figure 2 accurately represent their molecular geometries.

All four species of Figure 2 are unsaturated (16-electron) five-coordinate distorted square-pyramidal metal complexes. In **2a** and **2b**, the C1═C2 separation of 1.41 Å is normal, despite the olefin fragment being rotated approximately halfway between the principal axes of the molecular coordinate system (defined by the Ru−Cl, Ru−Hru, and P1−Ru−P2 bonds) and thus being, theoretically, unable to receive efficient back-donation from the nonbonding metal d_π orbitals. In **2a** and **2b**, the N1−C1and C3−N2 distances are the same (1.45 Å) and correspond to pure σ C−N bonds.

The alkylidene complex **2c** and carbene **2d** possess short Ru═C bonds of 1.87 and 1.90 Å, respectively. In the latter case, the N1−C1 bond of 1.37 Å is also short, consistent with partial double N−C bonding expected in a Fischer carbene. In **2d**, the Hru···H_a distance = 2.83 Å is in agreement with the observation

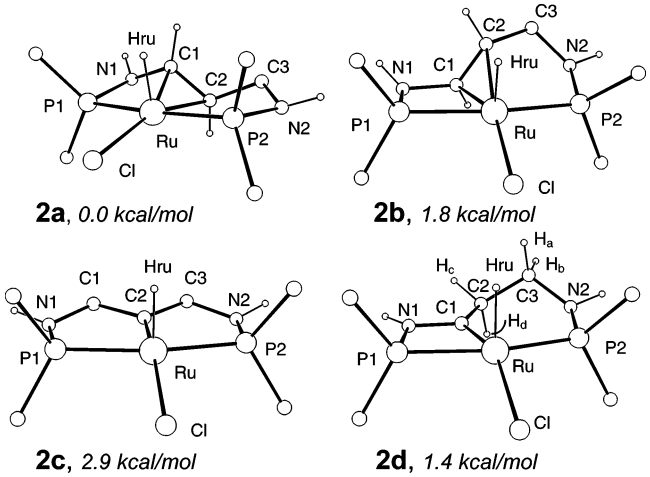

Figure 2. Calculated structures of complexes **2a**−**d**. All CH_3 groups and some hydrogen atoms have been omitted for clarity. Selected bond distances [Å] and angles [deg]: (**2a**) Ru−Hru 1.53, Ru−C1 2.156, Ru−C2 2.151, Ru−P1 2.358, Ru−P2 2.343, Ru−Cl 2.402, C1−C2 1.409, N1−C1 1.451, N2−C3 1.454, C2−Ru−Hru 104.3, Hru−Ru−Cl 94.2, P1−Ru−P2 173.0, C2−Ru−Cl 159.9, C1−C2−Ru−Hru 52.8; (**2b**) Ru−Hru 1.53, Ru−C1 2.113, Ru−C2 2.177, Ru−P1 2.355, Ru−P2 2.327, Ru−Cl 2.388, C1−C2 1.412, N1−C1 1.453, N2−C3 1.456, C2−Ru−Hru 75.2, Hru−Ru−Cl 95.3, P1−Ru−P2 167.0, C2−Ru−Cl 169.7, C1−C2−Ru−Hru 35.8; (**2c**) Ru−Hru 1.55, Ru−C2 1.867, Ru−P1 2.330, Ru−P2 2.330, Ru−Cl 2.432, N1−C1 1.444, C2−Ru−Hru 84.6, Hru−Ru−Cl 110.0, P1−Ru−P2 167.8, C2−Ru−Cl 165.3, Ru−C2−C1−C3 176.8; (**2d**) Ru−Hru 1.56, Ru−C1 1.902, Ru−P1 2.366, Ru−P2 2.301, Ru−Cl 2.442, N1−C1 1.370, N2−C3 1.454, C1−Ru−Hru 82.7, Hru−Ru−Cl 121.4, P1−Ru−P2 162.0, C1−Ru−Cl 153.4, N1−C1−Ru 110.1, C2−C1−Ru 133.8, N1−C1−C2 116.1, $H_b-C2-C3-H_c$ 60.0, $H_b-C2-C3-H_d$ 65.6.

Chart 5

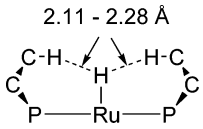

of an NOE between the two protons. No NOE could be observed between Hru and H_c, which are relatively far (3.90 Å) apart. Further in agreement with the observed $^3J_{H-H}$ coupling, the dihedral angles H_b—C3—C2—H_c = 60.0° and H_b—C3—C2—H_d = 65.6° are similar. An interesting feature observed for all isomers **2a**−**d** are the relatively close C—H···H—Ru contacts ranging from 2.11 to 2.28 Å as schematically shown in Chart 5.[6]

Calculated Gibbs free energies of isomers **2a**−**d** are given in Figure 2. The theoretical values are only slightly (0.4 to 1.5 kcal/mol) exaggerated relative to the experimental data. The calculations have correctly determined that (i) complexes **2a** and **2c** are the most and the least stable isomers, respectively, and (ii) complexes **2b** and **2d** have very similar energies differing by only 0.4 kcal/mol theoretically vs the experimental difference of 0.1 kcal/mol.

Encouraged by the success of the calculations on the ground-state geometries of **2a**−**d**, we also probed the mechanisms of the isomerization reactions of these complexes. All calculations were first carried out on a singlet ($S = 0$) potential energy surface, assuming that all intermediate species could be diamagnetic. The optimized intermediate and transition structures are presented in Figure 3, arranged in two series, each involving reversible β- and α-H elimination reactions: **2a** ⇄ **TS1** ⇄ **IN1** ⇄ **TS2** ⇄ **2c** and **2b** ⇄ **TS3** ⇄ **IN2** ⇄ **TS4** ⇄ **2d**. The two series are probably connected by isomerization of the olefin complexes **2a** ⇄ **2b**; however the mechanism of this process is not clear and, since it is a high energy process, may involve bond cleavage such as reversible dissociation of a PBu^t_2 group.

The central species of Figure 3 are nonplanar 14-electron intermediates **IN1** and **IN2**. They are related to the three crystallographically characterized *trans*-diphosphine 14-electron cationic complexes:[7,8] $[RuH(CO)L_2]^+$,[7a,d] $[Ru(Ph)(CO)L_2]^+$,[7b] and $[Ru(CH{=}CPh(SiMe_3))(CO)L_2]^+$[7c] (L = $PMeBu^t_2$), the latter two of which have a sawhorse geometry with ∠C—Ru—CO = 93°−94°. In the crystalline state, the complex cations were stabilized by agostic bonding of methyl (and in one case phenyl) C—H bonds; however, these interactions apparently did not play a major role. Indeed, the calculated structures of the diamagnetic species devoid of agostic bonding, $[RuH(CO)(PH_3)_2]^+$,[7a] $RuHCl(PH_3)_2$,[9] and $RuCl_2(PH_3)_2$,[8c] were also nonplanar.[10] The optimized structure of **IN2** possesses an agostic C—H bond, and that of **IN1** does not show agostic bonding.

The greater stability of nonplanar vs square-planar geometry for four-coordinate 14-electron d^6 metal systems has been attributed to a favorable large HOMO−LUMO gap in the sawhorse structure where the empty orbitals are strongly antibonding with the ligands.[7a,8c] However, it has been recently demonstrated that the 14-electron complex $RuCl[N(SiMe_2CH_2PBu^t_2)_2]$ is paramagnetic (triplet, $S = 1$) and has a square-planar ground state.[11] Apparently, the structure of 14-electron, four-coordinate d^6 diphosphine complexes of ruthenium can be either sawhorse (singlet, $S = 0$) in the presence of π-acceptor ligands and/or when the phosphines can adopt a cis-configuration or square-planar (triplet, $S = 1$) when the phosphines bind in a *trans*-fashion and there is no π-acceptor ligand on the metal. The intermediates **IN1** and **IN2** belong to the latter case; therefore, we conducted a wave function stability calculation for **IN1**, which indeed indicated that a lower energy nonsinglet structure existed for this complex. The triplet $RuCl[CH(C_2H_4PBu^t_2)_2]$ (**IN1triplet**) was optimized in an unrestricted DFT calculation, and the resulting geometry is shown in Figure 4. The structure can be described as slightly distorted square-planar (∠C2−Ru−Cl = 164.8° vs ∠C2−Ru−Cl = 125.7° in **IN1**) and is relatively low in energy, lying only 4.0 kcal/mol above **2a** and as much as 18.9 kcal/mol below **IN1**. Additionally, we carried out single-point unrestricted energy calculations for **TS1** and **TS2** (optimized as singlets) on the triplet PES. The electronic energy of the triplet **TS1** was found to be 5.7 kcal/mol above the singlet, and that of the triplet **TS2** was 12.4 kcal/mol below the singlet state. Chart 6 shows the reaction profile for the isomerization **2a** ⇄ **2c** on the singlet PES as a solid line, whereas the points corresponding to the triplet species are connected by a dashed line.

Along the singlet reaction path in Chart 6, β- and α-H elimination in the intermediate complex **IN1** lead to formation of the olefin and carbene products **2a** and **2c** via transition complexes **TS1** and **TS2**, respectively. The main features of the reaction profile connecting isomers **2b** and **2d** are qualitatively similar to those of Chart 6 (see Figure 3). Transition structure **TS1** is 25.8 kcal/mol above **2a** and represents an energy barrier close to the experimental value, $\Delta G^{\ddagger} = 24.6$ kcal/mol, deter-

(6) For discussions of M−H···H−C hydrogen bonding, see: (a) Richardson, T. B.; Koetzle, T. F.; Crabtree, R. H. *Inorg. Chim. Acta* **1996**, *250*, 69. (b) Xu, W.; Lough, A. J.; Morris, R. H. *Can. J. Chem.* **1997**, *75*, 475. (c) Patel, B. P.; Wessel, J.; Yao, W. B.; Lee, J. C.; Peris E.; Koetzle, T. F.; Yap, G. P. A.; Fortin, J. B.; Ricci, J. S.; Sini, G.; Albinati, A.; Eisenstein, O.; Rheingold, A. L.; Crabtree, R. H. *New J. Chem.* **1997**, *21*, 413.

(7) (a) Huang, D.; Huffman, J. C.; Bollinger, J. C.; Eisenstein, O.; Caulton, K. G. *J. Am. Chem. Soc.* **1997**, *119*, 7398. (b) Huang, D. J.; Streib, W. E.; Bollinger, J. C.; Caulton, K. G.; Winter, R. F.; Scheiring T *J. Am. Chem. Soc.* **1999**, *121*, 8087. (c) Huang, D. J.; Folting, K.; Caulton, K. G. *J. Am. Chem. Soc.* **1999**, *121*, 10318. (d) Huang, D. J.; Bollinger, J. C.; Streib, W. E.; Folting, K.; Young, V., Jr.; Eisenstein, O.; Caulton, K. G. *Organometallics* **2000**, *19*, 2281.

(8) There are other crystallographically characterized examples of diamagnetic, nonplanar 14-electron ruthenium complexes which possess two *cis*-coordinated phosphines, only one phosphine, or no phosphorus ligand: $Ru(SC_6F_5)_2(PPh_3)_2$,[8a−b] $RuCl_2[PPh_2(2,6\text{-}Me_2C_6H_3)]_2$,[8c] $Ru(O^tBu)_2(=CHPh)(PCy_3)$,[8d] $RuCl_2(BTZ)_2$[8e] (where BTZ is an imidazole derivative). (a) Catalá, R.-M.; Cruz-Garritz, D.; Terreros, P.; Torrens, H.; Hills, A.; Hughes, D. L.; Richards, R. L. *J. Organomet. Chem.* **1987**, *328*, C37. (b) Catalá, R.-M.; Cruz-Garritz, D.; Sosa, P.; Terreros, P.; Torrens, H.; Hills, A.; Hughes, D. L.; Richards, R. L. *J. Organomet. Chem.* **1989**, *359*, 219. (c) Baratta, W.; Mealli, C.; Herdtweck, E.; Ienco, A.; Mason, S. A.; Rigo, P. *J. Am. Chem. Soc.* **2004**, *126*, 5549. (d) Sandford, M. S.; Henling, L. M.; Day, M. W.; Grubbs, R. H. *Angew. Chem., Int. Ed.* **2000**, *39*, 3451. Sánchez-Delgado, R. A.; Navarro, M.; Lazardi, K.; Atencio, R.; Capparelli, M.; Vargas, F.; Urbina, J. A.; Bouillez, A.; Noels, A. F.; Masi, D. *Inorg. Chim. Acta* **1998**, *275*−*276*, 528.

(9) (a) Oliván, M.; Clot, E.; Eisenstein, O.; Caulton, K. G. *Organometallics* **1998**, *17*, 3091. (b) Gérad, H.; Clot, E.; Giessner-Prettre, C.; Caulton, K. G.; Davidson, E. R.; Eisenstein, O. *Organometallics* **2000**, *19*, 2291. (c) Volland, M. A. O.; Hofmann, P. *Helv. Chim. Acta* **2001**, *84*, 3456. (d) Dolker, N.; Frenking, G. *J. Organomet. Chem.* **2001**, *617*−*618*, 225.

(10) Our DFT calculations for $RuHCl(PH_3)_2$ and $RuCl_2(PH_3)_2$ at the *m*PW1PW91/6-311+g(d,p) level (using the SDD basis set for Ru) have found that the diamagnetic structures reported in the original publications[9a,b,8c] do not represent their ground states. The ground-state structure of $RuCl_2(PH_3)_2$ is square-planar and paramagnetic ($S = 1$) and is lower in energy than the nonplanar diamagnetic isomer by 2.2 kcal/mol. For $RuHCl(PH_3)_2$, the calculated structure published by Caulton and co-workers[9a,b] is by 4.1 kcal/mol higher in energy than the square-planar paramagnetic isomer and by 13.8 kcal/mol higher than the ground-state diamagnetic structure where the hydride and one phosphine are trans to the empty coordination sites, in agreement with the work in ref 9c, d. Predicting the structural and spin-state preferences of the molecules of this type can be difficult without careful and accurate calculations.

(11) (a) Watson, L. A.; Ozerov, O. V.; Pink, M.; Caulton, K. G. *J. Am. Chem. Soc.* **2003**, *125*, 8426. (b) Walstrom, A. N.; Watson, L. A.; Pink, M.; Caulton, K. G. *Organometallics* **2004**, *23*, 4814.

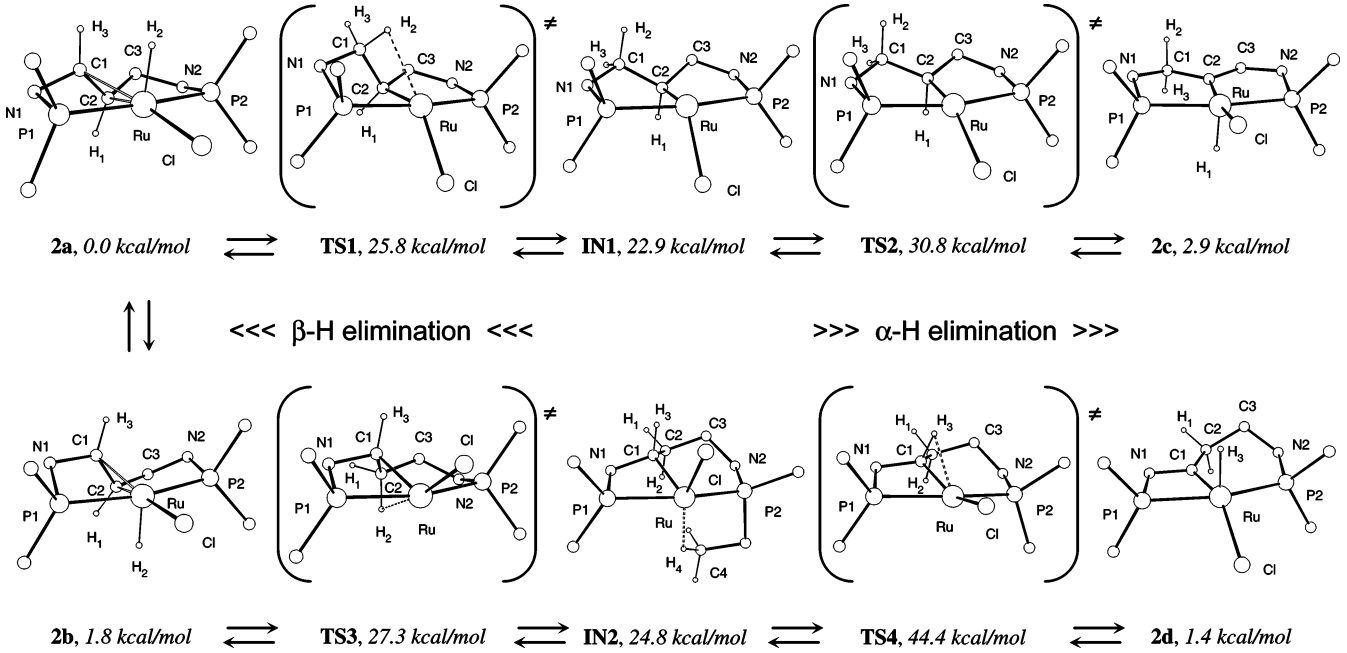

Figure 3. Calculated intermediate and transition structures connecting complexes **2a**−**d**. The CH_3 groups and some hydrogen atoms are not shown for clarity. Selected distances [Å] and angles [deg]: (**IN1**) Ru−C2 2.081, C2−H1 1.10, C2−Ru−Cl 125.7, H1−C2−Ru 106.2; (**IN2**) Ru−C1 2.064, Ru−H4 2.04, Ru−C4 2.817, C4−H4 1.13, C1−Ru−Cl 101.0, H3−C1−Ru 104.0; (**TS1**) Ru−C2 2.059, Ru−C1 2.542, Ru−H2 2.35, C1−H2 1.13, C2−Ru−Cl 132.6, Ru−C2−C1−H2 44.3; (**TS2**) C2−Ru 2.055, C2−H1 1.12, Ru−H1 2.30, H1−C2−Ru 87.5, C2−Ru−Cl 157.0; (**TS3**) Ru−C1 2.038, Ru−C2 2.843, Ru−H2 2.79, C2−H2 1.10, C1−Ru−Cl 120.7, Ru−C1−C2−H2 40.9; (**TS4**) C1−Ru 2.018, C1−H3 1.14, Ru−H3 2.15, H3−C1−Ru 80.7, C1−Ru−Cl 149.2.

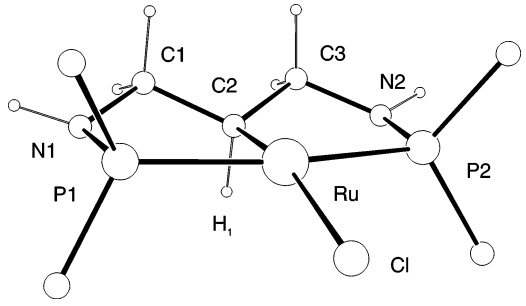

Figure 4. The optimized geometry of the 14-electron, square-planar RuCl-[$CH(C_2H_4PBu^t_2)_2$] (**IN1triplet**). For clarity, the CH_3 groups are not shown. Selected bond distances [Å] and angles [deg]: Ru−C1 2.093, Ru−Cl 2.434, Ru−P1 2.345, C2−H1 1.106, P1−Ru−P2 164.9, C2−Ru−Cl 164.8, H1−C2−Ru 98.1.

Chart 6

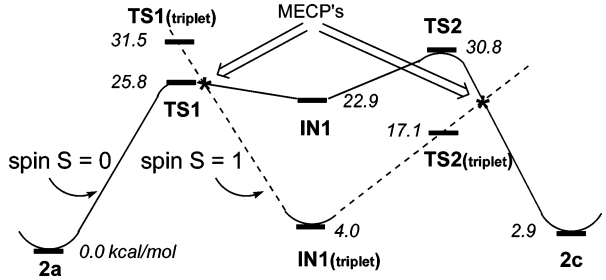

mined by NMR spectroscopy for the isomerization of **2a** into **2c** in THF-d_8. The theoretical rate-limiting step for the isomerization on the singlet PES is the α-elimination reaction with the transition state **TS2** at 30.8 kcal/mol, i.e., significantly exceeding the experimental activation energy. This and the low energy of the 14-electron species RuCl[$CH(C_2H_4PBu_2)_2$] on the triplet PES (dashed line in Chart 6) suggest that the isomerization reaction **2a** ⇄ **2c** should very likely involve a change in spin.[12] One MECP (minimum energy crossing point) on the reaction path can be close to transition structure **TS1**, which has a reasonably low energy on the singlet PES. The other MECP is probably situated in the region between **TS2** and **2c**, at an energy well below that of **TS2**.

Part 2, Reaction of L2. Attempts to prepare olefin or carbene complexes RuHCl[2,6-$(CH_2PBu^t_2)_2C_6H_8$] (**3**) by reacting 1,3-bis(di-*tert*-butylphosphinomethyl)cyclohexane (**L2**) with [$RuCl_2$-(*p*-cymene)]$_2$ under nitrogen were unsuccessful. When this reaction was carried out under hydrogen, it cleanly afforded the dihydride RuH_2Cl[2,6-$(CH_2PBu^t_2)_2C_6H_9$] (**4**) according to Scheme 4. The crystal structure of complex **4** was established by X-ray analysis and will be discussed in the following section.

Heating a THF solution of **4** resulted in dehydrogenation and formation of two olefin compounds **3a** and **3b** along with carbene complexes **3c** and **3c′** shown in Chart 7. A 95% conversion of **4** was achieved after 16 h (monitored by ^{31}P NMR), and the red-brown product containing **3c** (58.4%), **3c′** (32.3%), and small amounts of **3a** (3.4%), **3b** (0.9%), and **4** (5.0%) was isolated in 79% yield. Five successive crystallizations of the product afforded a solid containing **3c** (83.5%), **3c′** (12.8%), and **4** (3.7%). The isomerization reactions of **3** were slow at room temperature. However, heating a toluene-d_8 solution of the recrystallized **3** for 1 h at 100 °C produced an equilibrium mixture of all four isomers: **3a** (10.7%), **3b** (4.3%), **3c** (47.0%), and **3c′** (38.0%). This mixture did not change after additional heating for 20 h.

A sample of crystalline **3** was submitted for an X-ray diffraction study, and the crystal picked out for analysis happened to

(12) Strong spin−orbit coupling interactions in the atoms of heavy elements such as transition metals most likely make reactions involving a change in spin not much different from those proceeding on a single potential energy surface. The subject was reviewed in: (a) Poli, R.; Harvey, J. N. *Chem. Soc. Rev.* **2003**, *32*, 1. (b) Harvey, J. N.; Poli, R.; Smith, K. M. *Coord. Chem. Rev.* **2003**, *238*−*239*, 347.

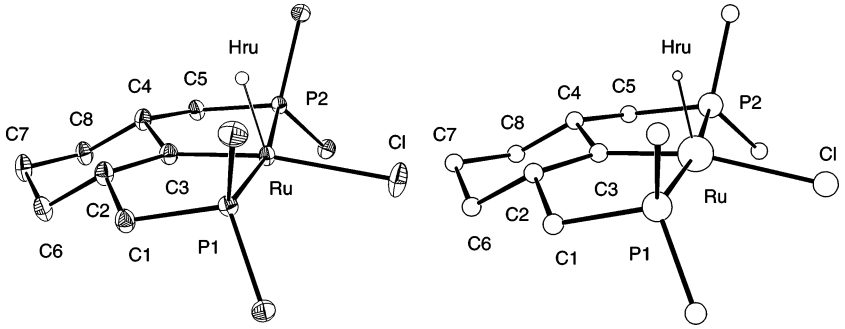

Figure 5. Experimental (left) and calculated (right) structures of **3c**. For clarity, all CH_3 groups and hydrogen atoms bonded to carbon are not shown. Thermal ellipsoids are drawn at 30% probability. Selected experimental bond distances [Å] and angles [deg]: Ru−Hru 1.56(4), Ru−C3 1.902(2), Ru−Cl 2.4461(6), Ru−P1 2.3232(5), Ru−P2 2.3350(5), C3−Ru−Hru 76.9(16), Hru−Ru−Cl 113.3(16), C3−Ru−Cl 169.77(8), P1−Ru−P2 168.92(2). Calculated bond distances [Å] and angles [deg]: Ru−Hru 1.55, Ru−C3 1.886, Ru−Cl 2.445, Ru−P 2.341, C3−Ru−Hru 82.1, Hru−Ru−Cl 111.6, C3−Ru−Cl 166.4, P1−Ru−P2 171.2.

Scheme 4 [a]

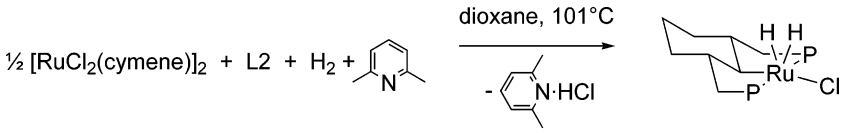

4

[a] P = PBu^t_2.

Chart 7. [a]

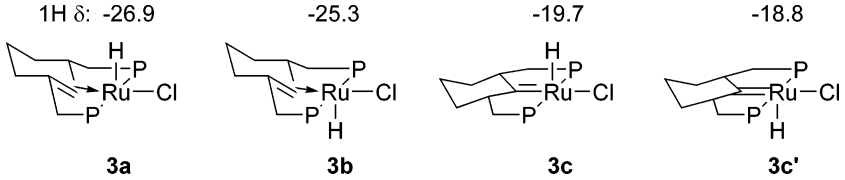

3a **3b** **3c** **3c'**

[a] P = PBu^t_2.

contain only **3c**. An ORTEP plot of **3c** is presented in Figure 5 together with a DFT structure of **3c**. A list of selected bond distances and angles is given in the figure's caption. The calculated and crystal structures agree well, and differences between the principal bond distances and angles are within 0.018 Å and 3.4°, respectively. The coordination environment of the C_s-symmetrical **3c** is best described as distorted square-pyramidal, with the hydride visibly displaced from the idealized apical position. This distortion (called Y-type distortion) is typical of five-coordinate 16-electron complexes containing a halide ligand and helps to enhance π-donation from the halide to the unsaturated metal center.[13] The molecule of **3c** has a short Ru−C3 = 1.902(2) distance, characteristic of a metal alkylidene, and a nearly planar C2−C3−C4−Ru fragment (the sum of the bond angles = 358.6°). The cyclohexane ring of **3c** adopts a chair conformation where the bulky $CH_2PBu^t_2$ substituents are equatorial and the axial C−H hydrogen atoms are syn with the hydride.

The $^{13}C\{^1H\}$ and ^{13}C DEPT NMR spectra of **3c** and **3c′** were well resolved and showed the same numbers of C, CH, CH_2, and CH_3 resonances. The C=Ru resonances appeared at δ 334.7 (t, $^2J_{CP}$ = 3.1 Hz, **3c**) and 334.4 (t, $^2J_{C-P}$ = 2.9 Hz, **3c′**), respectively, as expected for alkylidene complexes. Single ^{31}P NMR chemical shifts for **3c** (δ 81.3) and **3c′** (δ 79.9) were in agreement with the overall C_s molecular symmetry. The hydride ligands of **3c** and **3c′** gave rise to triplets at δ −19.7 ($^2J_{H-P}$ = 17.1 Hz) and −18.8 ($^2J_{H-P}$ = 17.7 Hz), respectively. In the ^1H NMR spectra, an NOE was observed between the hydride at δ −19.7 and the 2 × CH resonance at δ 0.69 (assigned with the help of a $^{13}C/^1H$ HETCOR experiment), indicating a syn arrangement observed in the crystal structure of **3c**. On the contrary, no NOE was detected between the δ −18.8 hydride and CH protons. These NMR observations confirm that the two isomers **3c** and **3c′** differ by orientation of their hydrides with respect to the PCP ligand plane.

Minor isomers **3a** and **3b** were assigned the structures according to Chart 7 based on the similarity of their key NMR properties to those of the crystallographically characterized olefin complexes **1a** and **1b**. Thus, the hydride patterns of **3a** and **3b** (benzene-d_6, δ −26.9 (ddd), $^2J_{HP}$ = 21.6, 15.9 Hz, $^3J_{HH}$ = 1.8 Hz and δ −25.3 (dd), $^2J_{HP}$ = 23.1, 15.9 Hz, respectively) are similar to those of **1a** and **1b** (in toluene-d_8, δ −27.8 (ddd), $^2J_{HP}$ = 21.9, 16.8 Hz, $^3J_{HH}$ = 2.1 Hz and δ −23.5 (dd), $^2J_{HP}$ = 20.1, 14.5 Hz, respectively). The ^{31}P NMR data are also similar for **3a** (δ −18.6, 82.6; $^2J_{PP}$ = 288 Hz) and **1a** (δ −22.9, 86.4; $^2J_{PP}$ = 289 Hz) and for **3b** (δ −13.8, 79.2; $^2J_{PP}$ = 292 Hz) and **1b** (δ −7.1, 84.0; $^2J_{PP}$ = 305 Hz).

We believe that the isomerization **3a** ⇄ **3c′** proceeds via a four-coordinate 14-electron intermediate and involves α- and β-H elimination reactions analogous to those discussed for the isomerization reactions of **2a** and **2c** and diagrammed in Figure 3 and Chart 6. The other two isomers, **3b** and **3c**, are most likely formed from **3a** and **3c′**, respectively, by hydride migration across the PCP plane, the process which may involve reversible dissociation of a PBu^t_2 group.

(13) Gerard, H.; Davidson, E. R.; Eisenstein, O. *Mol. Phys.* **2002**, *100*, 533.

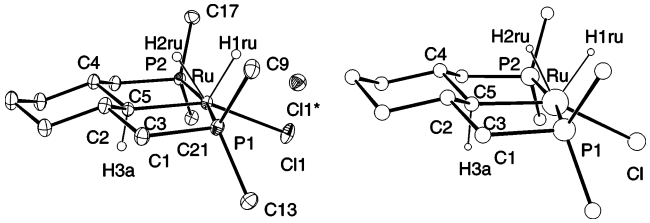

Figure 6. Experimental (left) and calculated (right) structures of **4**. For clarity, all CH_3 groups and most of the hydrogen atoms bonded to carbon are not shown. Thermal ellipsoids are drawn at 30% probability. Selected experimental bond distances [Å] and angles [deg]: Ru−H1ru 1.48(3), Ru−H2ru 1.50(3), H1ru−H2ru 1.56, Ru−C3 2.080(2), Ru−Cl 2.4429(6), Ru−P1 2.3492(6), Ru−P2 2.3393(6), C3−Ru−H2ru 59.8(9), H2ru−Ru−H1ru 62.8(14), H1ru−Ru−Cl 83.0(11), C3−Ru−Cl 154.39(6), P1−Ru−P2 166.45(2). Calculated bond distances [Å] and angles [deg]: complex **4**, Ru−H1ru 1.54, Ru−H2ru 1.54, H1ru−H2ru 1.54, Ru−C3 2.091, Ru−Cl 2.427, Ru−P 2.358, C3−Ru−H2ru 63.7, H2ru−Ru−H1ru 59.9, H1ru−Ru−Cl 83.1, C3−Ru−Cl 153.2, P1−Ru−P2 167.6.

Part 3, Hydrogenation of 2 and 3. The isomers of **3** reacted with hydrogen within minutes in solution to regenerate the dihydride **4** as the sole product. The solid-state structure of **4** was determined by X-ray analysis. An ORTEP plot of the complex is presented in Figure 6 together with a calculated structure of **4**; selected bond distances and angles are listed in the figure's caption. The crystal structure of **4** shows a disordered chloride which can be due to the presence of a small amount of an isomer of **3** cocrystallized with **4**. The H1ru···H2ru experimental and calculated distances of 1.56 and 1.54 Å, respectively, are somewhat short but nevertheless consistent with a Ru(IV) dihydride formulation. The molecule of **4** has an irregular C_s symmetrical geometry which is best described as a pentagonal bipyramid missing an equatorial ligand. The empty coordination site of this 16-electron complex is situated between the chloride and the metal-bonded carbon ($\angle$Cl−Ru−C3 = 154.4°). This arrangement is very similar to those found in the related 16-electron osmium dihydrides, $[OsH_2Cl(1,5\text{-}(PBu^t_2)_2C_5H_9)]$[4] and $[OsH_2Cl(2,6\text{-}(CH_2PBu^t_2)_2C_6H_3)]$.[14] In general, large deviations from an octahedral geometry are common for diamagnetic six-coordinate d^4 metal complexes.[9d,15] The small angle $\angle$Ru−C3−H3a = 94.3° and an elongated bond C3−H3a = 1.118 Å in the calculated structure of **4** suggested a weak α-agostic interaction between the C3−H3a bond and ruthenium. Indeed, a reduced C−H coupling of 112.9 Hz was observed for the (CH)Ru fragment in a proton coupled ^{13}C NMR spectrum. Saturation of a benzene-d_6 solution of **4** with deuterium gas for several minutes led to complete deuteration of H3a and the hydride sites, indicating an exchange process involving α-H elimination.

We also studied hydrogenation of **2** in solution, which cleanly produced the dihydride $RuH_2Cl[CH(CH_2NHPBu^t_2)_2]$ (**5**) within 15 min. The conversion was close to quantitative; however, trace amounts of the isomers of **2** remained even after a prolonged exposure to hydrogen, indicating the thermodynamic instability of **5**. Therefore, we did not try isolation of the dihydride **5** and characterized this complex by solution NMR techniques. A structure of **5** was optimized in a DFT calculation and is shown in Figure 7. All bond distances and angles in the first coordination sphere of the calculated species **4** and **5** compare well and do not exhibit noteworthy differences.

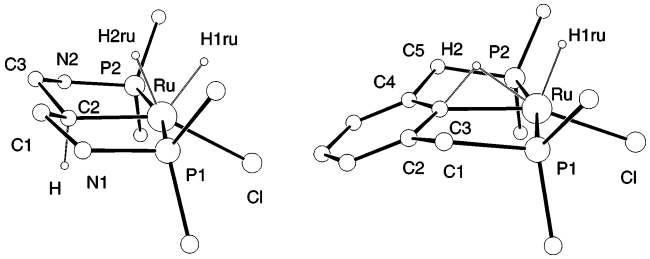

Figure 7. Calculated structures of complexes **5** (left) and **6** (right). For clarity, all CH_3 groups and most of the hydrogen atoms are not shown. Calculated bond distances [Å] and angles [deg]: Complex **5**, Ru−H1ru 1.54, Ru−H2ru 1.54, H1ru−H2ru 1.53, Ru−C2 2.076, Ru−Cl 2.420, Ru−P 2.340, C2−H 1.111, C2−Ru−H2ru 65.6, H2ru−Ru−H1ru 59.7, H1ru−Ru−Cl 82.9, C2−Ru−Cl 151.8, P1−Ru−P2 165.9, H−C2−Ru 94.2. Complex **6**, Ru−H1ru 1.54, Ru−H2 1.67, H1ru−H2 1.90, Ru−C3 2.130, Ru−Cl 2.389, Ru−P 2.351, C3−H2 1.258, C3−Ru−H2ru 36.1, H2−Ru−H1ru 72.6, H1ru−Ru−Cl 91.0, C3−Ru−Cl 160.3, P1−Ru−P2 166.9.

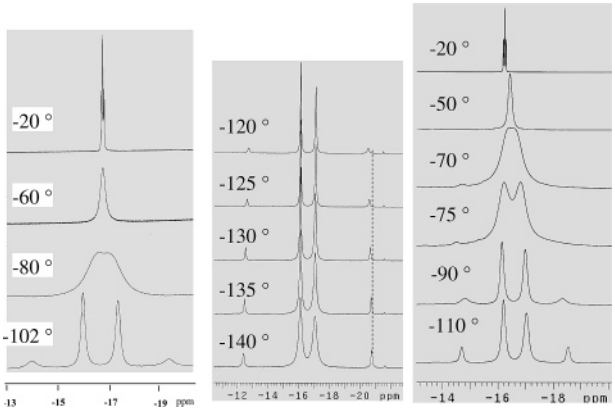

Figure 8. VT ^1H NMR spectra of **4** in CD_2Cl_2 (left), $^1H\{^{31}P\}$ NMR spectra of **4** in $CDFCl_2$ (center), and ^1H NMR spectra of **5** in CD_2Cl_2 (right).

It is interesting to compare dihydrides **4**, **5** and a related η^2-CH agostic complex, RuHCl[1,3-$(CH_2PBu^t_2)_2C_6H_4$] (**6**). A DFT calculated structure of **6** is shown in Figure 7 and exhibits an elongated C3−H2 bond of 1.26 Å, in agreement with the experimental distance, 1.31(5) Å, determined by X-ray diffraction.[16] The Ru−H2 separation is 1.67 Å. The corresponding distances in dihydride **4** are C3−H2ru = 1.97 and Ru−H2ru = 1.54 Å. It is obvious that $[2,6\text{-}(CH_2PBu^t_2)_2C_6H_9]^-$ is a better donor than $[2,6\text{-}(CH_2PBu^t_2)_2C_6H_3]^-$, and the latter is unable to support Ru(IV). A related observation has been recently made for the iridium complexes $Ir(NH_3)[1,3\text{-}(CH_2PBu^t_2)_2C_6H_3]$ and $IrH(NH_2)[1,5\text{-}(CH_2PBu^t_2)_2C_5H_9]$, possessing Ir(I) and Ir(III) centers, respectively.[17]

In a ^1H NMR spectrum, the two inequivalent hydrides of **4** rapidly exchanged sites at 20 °C and appeared as a triplet at −16 ppm in CD_2Cl_2. This signal decoalesced at −80 °C to become an AB system at −100 °C (δ −15.0, −18.4) exhibiting a quantum exchange coupling[18] of 628 Hz between the hydrides (Figure 8, left). The temperature dependence of **5** was similar, and an exchange coupling of 453 Hz was observed at −110 °C between the inequivalent hydrides at δ −15.71 and −17.50. Using a low-boiling solvent, $CDFCl_2$, we were able to study

(14) Gusev, D. G.; Dolgushin, F. M.; Antipin, M. Yu. *Organometallics* **2001**, *20*, 1001.
(15) Gusev, D. G.; Kuhlman, R.; Rambo, J. R.; Berke, H.; Eisenstein, O.; Caulton, K. G. *J. Am. Chem. Soc.* **1995**, *117*, 281.
(16) Gusev, D. G.; Madott, M.; Dolgushin, F. M.; Lyssenko, K. A.; Antipin, M. Yu. *Organometallics* **2000**, *19*, 1734.
(17) Zhao, J.; Goldman, A. S.; Hartwig, J. F. *Science* **2005**, *307*, 1080.
(18) (a) Heinekey, D. M.; Hinkle, A. S.; Close, J. D. *J. Am. Chem. Soc.* **1996**, *118*, 5353. (b) Sabo-Etienne, S.; Chaudret, B. *Chem. Rev.* **1998**, *98*, 2077. (c) Kuhlman, R.; Clot, E.; Leforestier, C.; Streib, W. E.; Eisenstein, O.; Caulton, K. G. *J. Am. Chem. Soc.* **1997**, *119*, 10153.

Chart 8

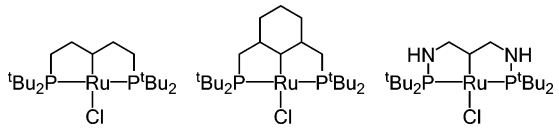

Chart 9

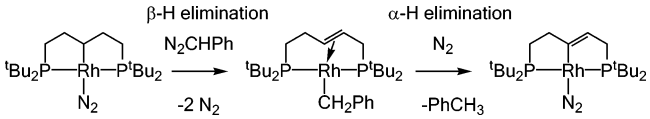

Chart 10

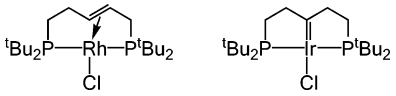

the temperature dependence of J_{H-H} for **4** below −100 °C. The coupling was found to be larger in $CDFCl_2$ than in CD_2Cl_2, and interestingly, it increased on lowering the temperature: 950 Hz (−110 °C), 974 Hz (−115 °C), 1024 Hz (−120 °C), 1051 Hz (−125 °C), 1078 Hz (−130 °C), 1098 Hz (−135 °C), 1110 Hz (−140 °C). Normally, quantum exchange couplings *decrease* with decreasing temperature. The only recorded exception to this is the 16-electron osmium trihydride complex, $OsH_3Cl(P^iPr_3)_2$.[18c] It is perhaps more than a coincidence that $OsH_3Cl(P^iPr_3)_2$, our compounds **4** and **5**, and the previously reported $RuH_2Cl[CH(C_2H_4PBu^t_2)_2]$[4] form a small group of 16-electron complexes known to show exchange coupling and that the osmium trihydride and **4** both have an inverse dependence of J_{H-H} on *T*. It was proposed in ref 18c that the unsaturation might allow rapid and reversible solvent coordination (even methylcyclohexane!) or weak intramolecular agostic bonding, and therefore the unusual temperature dependence of J_{H-H} could be due to chemical changes in the system. It is difficult to argue against this but is difficult to furnish supporting experimental evidence. We should leave the question about the origin of the unusual dependence of J_{H-H} on *T* in 16-electron hydride complexes open until new experimental and theoretical data provide definitive clues.

Concluding Remarks. This and our previous[3,4] works have established that the 14-electron four-coordinate $Ru^{(II)}Cl(PCP)$ species diagramed in Chart 8 are capable of extensive C−H activation and H-elimination from the cyclometalated pincer ligand backbone, affording olefin and carbene products under mild conditions and upon heating. There are certain analogies between the chemistry of our pincer complexes of group 8 metals and those of the metals from group 9, rhodium and iridium. One example of this is the work of Vigalok and Milstein who reported a sequence of α- and *β*-H elimination reactions depicted in Chart 9.[19] Another example is the olefin Rh(I) compound in Chart 10 (analogous to **1a** and **1b**) which was found in a mixture of products obtained by reaction of $RhCl_3$ with 1,5-bis(di-*tert*-butylphosphino)pentane by Shaw and coworkers.[20] In the case of the 5d metals, both the iridium complex[21] $IrCl[=C(C_2H_4PBu^t_2)_2]$ (Chart 10) and its osmium analogue, $OsHCl[=C(C_2H_4PBu^t_2)_2]$,[4] exist as alkylidenes, in line with the preference of 5d metals for higher oxidation states.

An unusual property of the ruthenium complexes in this work is the relative flatness of the potential energy surface on which all possible olefin and carbene isomers accessible through α- and *β*-H eliminations coexist in equilibrium. A special feature of these observable diamagnetic systems is that the key 14-electron intermediates involved (Chart 8) should be paramagnetic. The related 14-electron paramagnetic complex, $RuCl[N(SiMe_2CH_2PBu^t_2)_2]$, has been recently isolated and has shown some fascinating "spin-forbidden" reactivity.[22] The traditional interpretation of reaction mechanisms in organometallic chemistry is usually done considering only diamagnetic species. This work adds an example when this is not the case. Although the 14-electron species, $Ir[2,6\text{-}(CH_2PR_2)_2C_6H_3]$ (R = Bu^t, Pr^i), implicated in the catalytic dehydrogenation of alkanes,[23] are apparently diamagnetic, unsaturated 4d and 5d late transition metal centers can be paramagnetic. For instance, the 16-electron $IrCp^*(PR_3)$, an important intermediate in C−H activation reactions, has a paramagnetic ground state.[24]

Experimental Section

General Considerations. All manipulations were performed under nitrogen using standard Schlenk techniques or in a drybox where the anhydrous solvents were stored and used. FT IR spectra were recorded on a Perkin-Elmer Spectrum BXII spectrometer. NMR measurements were done on a Varian UNITY Inova 300 spectrometer. Throughout this paper, the NMR data are reported with the apparent coupling of observed virtual triplets (vt) denoted as $^{\nu}J$. All chemicals were obtained from Aldrich. Ligands **L1** and **L2** were prepared according to published methods.[25]

$RuHCl[Bu^t_2PNHC_3H_4NHPBu^t_2]$ (2). A mixture of $[RuCl_2(p\text{-cymene})]_2$ (1.5 g, 4.9 mmol), 1,3-bis(*N*-(di-*tert*-butylphosphino)amino)-propane (1.8 g, 5.0 mmol) and triethylamine (0.56 g, 5.5 mmol) in toluene (10 mL) was warmed for 1.5 h at 80 °C. The solvent was reduced in volume to 2 mL that resulted in precipitation of a brick-red solid. The precipitate was filtered, washed with methanol, and dried under a vacuum. The combined mother liquor and washings were evaporated to dryness. Addition of 3 mL of methanol and stirring the mixture for 30 min afforded a second crop of the product. The solid was filtered, washed with 3 × 1 mL of methanol, and dried under a vacuum. Total yield: 1.84 g (76%). Anal. Calcd for $C_{19}H_{43}ClN_2P_2Ru$: C, 45.82; H, 8.70; N, 5.62. Found: C, 45.90; H, 8.70; N, 5.41. Isomer **2a**. IR (Nujol): ν(RuH) 2117 cm^{-1}, ν(NH) 3260 cm^{-1}. ^1H NMR (CD_2Cl_2): δ −28.20 (ddd, $^2J_{HP}$ = 21.6, 17.1 Hz, $^3J_{HH}$ = 2.3 Hz, 1H, Ru*H*). $^1H\{^{31}P\}$ NMR: δ 1.07, 1.11, 1.42, 1.45 (s, 4 × 9H, CH_3), 1.97 (dd, J_{HH} = 9.9, 8.0 Hz, 1H, CH_2), 2.04 (s, 1H, N*H*), 3.68 (s, 1H, N*H*), 3.74 (dd, J_{HH} = 9.8, 6.2 Hz, 1H, CH_2), 4.01 (tdd, $^3J_{HH}$ = 7.0, 6.2, 2.3 Hz, 1H, =C*H*), 4.18 (d, $^3J_{HH}$ = 7.0 Hz, 1H, =C*H*). $^{31}P\{^1H\}$ NMR: δ 37.2, 131.1 (d, $^2J_{PP}$ = 289 Hz). $^{13}C\{^1H\}$ NMR: δ 27.80, 28.07, 28.27, 28.31 (dd, 4 × CH_3), 36.3 (dd, J_{CP} = 7.0, 4.4 Hz, P*C*), 37.4 (dd, J_{CP} = 3.7, 1.7 Hz, P*C*), 38.3 (dd, J_{CP} = 11.9, 4.0 Hz, P*C*), 39.7 (dd, J_{CP} = 17.0,

(19) Vigalok, A.; Milstein, D. *Organometallics* **2000**, 19, 2061.
(20) Crocker, C.; Errington, R. J.; Markham, R.; Moulton, C. J.; Odell, K. J.; Shaw, B. L. *J. Am. Chem. Soc.* **1980**, *102*, 4373.
(21) Crocker, C.; Empsall, H. D.; Errington, R. J.; Hyde, E. M.; McDonald, W. S.; Markham, R.; Norton, M. C.; Shaw, B. L.; Weeks, B. *J. Chem. Soc., Dalton Trans.* **1982**, 1217.
(22) (a) Watson, L. A.; Pink, M.; Caulton, K. G. *J. Mol. Catal. A: Chem.* **2004**, *224*, 51. (b) Walstrom, A.; Pink, M.; Yang, X.; Tomaszewski, J.; Baik, M.-H.; Caulton, K. G. *J. Am. Chem. Soc.* **2005**, *127*, 5330. (c) Ingleson, M. J.; Yang, X.; Pink, M.; Caulton, K. G. *J. Am. Chem. Soc.* **2005**, *127*, 10846. (d) Walstrom, A.; Pink, M.; Tsvetkov, N. P.; Fan, H.; Ingleson, M.; Caulton, K. G. *J. Am. Chem. Soc.* **2005**, *127*, 16780.
(23) (a) Krogh-Jespersen, K.; Czerw, M.; Summa, N.; Renkema, K. B.; Achord, P. D.; Goldman, A. S. *J. Am. Chem. Soc.* **2002**, *124*, 11404. (b) Renkema, K. B.; Kissin, Y. V.; Goldman, A. S. *J. Am. Chem. Soc.* **2003**, *125*, 7770. (c) Zhu, K. M.; Achord, P. D.; Zhang, X. W.; Krogh-Jespersen, K.; Goldman, A. S. *J. Am. Chem. Soc.* **2004**, *126*, 13044.
(24) Smith, K. M.; Poli, R.; Harvey, J. N. Chem.-Eur. J. 2001, 7, 1679.
(25) (a) Kuchen, W.; Peters, W.; Suenkeler, M. *J. Prakt. Chem.* **1999**, *341*, 182. (b) Kuznetsov, V. F.; Lough, A. J.; Gusev, D. G. *Inorg. Chim. Acta* **2006**, *359*, 2806.

4.0 Hz, P*C*), 48.8 (d, J_{CP} = 12.5 Hz, *C*H_2), 64.7 (dd, J_{CP} = 15.2, 1.1 Hz, =*C*H), 73.9 (t, J_{CP} = 1.6, =*C*H). Isomer **2b**, ^{1}H NMR (CD_2Cl_2): δ −24.23 (ddd, $^2J_{HP}$ = 21.6, 17.4 Hz, $^3J_{HH}$ = 2.6 Hz, 1H, Ru*H*). ^{31}P-{^{1}H} NMR: δ 50.1, 130.7 (d, $^2J_{PP}$ = 305 Hz). ^{13}C{^{1}H} NMR: δ 47.5 (d, J_{CP} = 10.8 Hz, *C*H_2), 60.9 (s, =*C*H), 70.9 (d, J_{CP} = 12.8 Hz, =*C*H). Isomer **2c**, ^{1}H NMR (CD_2Cl_2): δ −20.18 (t, $^2J_{HP}$ = 17.7 Hz, 1H, Ru*H*). ^{31}P{^{1}H} NMR: δ 133.7 (s). ^{13}C{^{1}H} NMR: δ 37.7 (t, $^vJ_{CP}$ = 8.9 Hz, P*C*), 39.4 (t, $^vJ_{CP}$ = 8.6 Hz, P*C*), 74.4 (t, $^vJ_{CP}$ = 11.8 Hz, *C*H_2), 318.0 (t, $^2J_{CP}$ = 6.4 Hz, Ru=*C*). Isomer **2d**, ^{1}H NMR (CD_2Cl_2): δ −22.23 (dd, $^2J_{HP}$ = 21.7, 15.9 Hz, 1H, Ru*H*). ^{1}H{^{31}P} NMR: δ 1.25, 1.28, 1.34, 1.40 (s, 4 × 9H, CH_3), 1.91 (m, 2H, CH_2), 2.00 (s, 1H, N*H*), 2.93 (ddd, J_{HH} = 12.3, 9.3, 4.0 Hz, 1H, CH_2), 3.20 (dt, J_{HH} = 12.3, 4.0 Hz, 1H, CH_2), 7.76 (s, 1H, N*H*). ^{31}P{^{1}H} NMR: δ 89.9, 107.4 (d, $^2J_{PP}$ = 300 Hz). ^{13}C{^{1}H} NMR (NMP): δ 44.8 (d, J_{CP} = 5.7 Hz, *C*H_2), 46.5 (dd, J_{CP} = 9.2, 3.8 Hz, *C*H_2), 275.0 (dd, $^2J_{CP}$ = 18.6, 10.0 Hz, Ru=*C*).

RuHCl[2,6-(CH$_2$PBu$^t_2$)$_2$C$_6$H$_8$] (3): A stirred solution of the dihydride **4** (0.5 g, 0.93 mmol) in a mixture of THF and dioxane (50:10 mL) was refluxed for 24 h. Then, the dark red solution was reduced in volume to ca. 8 mL and set aside for 2 h. A solid crystallized and was separated by filtration, washed with hexane (3 × 2 mL), and dried under a vacuum to give **3** (0.34 g, red-brown crystals). An additional 50 mg of the complex was isolated from the mother liquor upon concentration. Total yield: 0.39 g (0.73 mmol, 79%). Anal. Calcd for $C_{24}H_{49}ClP_2Ru$: C, 53.77; H, 9.21. Found: C, 53.67; H, 9.02. ^{31}P{^{1}H} NMR (C_6D_6) δ: 81.3 (s, isomer **3c**), 79.9 (s, isomer **3c′**). ^{1}H NMR (C_6D_6) δ: isomer **3c**, −19.67 (t, ^2J = 17.7 Hz, 1H, Ru*H*), 0.68 (m, 1H), 1.17−1.57 (CH_3, **3c** and **3c′** overlapped), 1.93 (m, 1H), 2.04 (m, 1H); isomer **3c′**, −18.77 (t, ^2J = 17.1 Hz), 1.05 (m, 1H), 1.17−1.57 (CH_3, **3c** and **3c′** overlapped), 1.62 (m, 2H), 1.79 (m, 1H), 2.16 (m, 1H). ^{13}C{^{1}H} NMR (C_6D_6), isomer **3c**, δ: 26.0 (vt, ^vJ = 1.9 Hz, *C*H_2), 29.5 (vt, ^vJ = 2.9 Hz, *C*H_3), 29.6 (vt, ^vJ = 3.2 Hz, *C*H_3), 30.9 (vt, ^vJ = 7.1 Hz, *C*H_2), 34.4 (vt, ^vJ = 7.5 Hz, *C*Me$_3$), 34.9 (vt, ^vJ = 5.9 Hz, *C*H_2), 36.2 (vt, ^vJ = 6.7 Hz, *C*Me$_3$), 71.2 (vt, ^vJ = 11.5 Hz, *C*H), 334.6 (t, J = 2.9 Hz, *C*=Ru); isomer **3c′**, δ: 26.2 (vt, ^vJ = 1.7 Hz, *C*H_2), 30.3 (vt, ^vJ = 2.9 Hz, *C*H_3), 30.4 (vt, ^vJ = 3.3 Hz, *C*H_3), 31.1 (vt, ^vJ = 6.9 Hz, *C*H_2), 34.1 (vt, ^vJ = 6.9 Hz, *C*Me$_3$), 35.4 (vt, ^vJ = 5.9 Hz, *C*H_2), 36.2 (vt, ^vJ = 6.2 Hz, *C*Me$_3$), 69.4 (vt, ^vJ = 11.2 Hz, *C*H); 334.4 (t, J = 3.1 Hz, *C*=Ru).

RuH$_2$Cl[2,6-(CH$_2$PBu$^t_2$)$_2$C$_6$H$_9$] (4): A stirred mixture of [RuCl$_2$(*p*-cymene)]$_2$ (0.57 g, 0.93 mmol), *cis*-1,3-bis(di-*tert*-butylphosphinomethyl)cyclohexane (0.78 g, 1.95 mmol), 2,6-lutidine (0.2 g, 1.86 mmol), and dioxane (10 mL) was heated to reflux for 12 h under hydrogen. The resulting dark orange solution was evaporated to dryness under a vacuum. The residue was extracted with THF (15 mL). The resulting solution was filtered, and the solid was washed with THF (3 × 4 mL). The combined filtrates were diluted with isooctane (12 mL), reduced in volume under a vacuum to ca. 10 mL, and set aside for 3 h. The precipitated product was filtered, washed with hexane (3 × 4 mL), and dried under a vacuum to give 823 mg of **4** as a light orange microcrystalline solid. An additional 63 mg of the complex was isolated from the mother liquor upon concentration. Total yield: 886 mg (1.65 mmol, 88%). Anal. Calcd for $C_{24}H_{51}ClP_2Ru$: C, 53.57; H, 9.55. Found: C, 53.65; H, 9.43. ^{31}P{^{1}H} NMR (C_6D_6), δ: 79.3 (s). ^{1}H NMR (C_6D_6), δ: −16.06 (t, J = 13.8 Hz, 2H), 0.91−1.52 (m, 5H), 1.14 (vt, ^vJ = 6.3 Hz, 18H), 1.34 (broad, 18H), 1.65−1.89 (m, 6H), 2.0 (m, 2H). ^{13}C{^{1}H} NMR (C_6D_6), δ: 26.96 (vt, ^vJ = 1.7 Hz, CH_2), 29.24 (broad, CH_3), 29.41 (vt, ^vJ = 3.2 Hz, CH_3), 32.61 (vt, ^vJ = 7.8 Hz, CH_2), 34.02 (vt, ^vJ = 7.4 Hz, CMe_3), 35.98 (vt, ^vJ = 7.2 Hz, CMe_3), 36.06 (vt, ^vJ = 7.7 Hz, CH_2), 54.77 (vt, ^vJ = 8.07 Hz, CH), 89.69 (s, CH).

RuH$_2$Cl[CH(CH$_2$NHPBu$^t_2$)$_2$] (5): This complex was prepared in solution by reacting **2** with hydrogen gas in a J. Young NMR tube. ^{1}H NMR (toluene-d_8): δ −15.99 (td, $^2J_{HP}$ = 14.6 Hz, $^3J_{HH}$ = 3.7 Hz, 2H, RuH_2). ^{1}H{^{31}P} NMR (toluene-d_8): δ 1.12, 1.29 (s, 2 × 18H, CH_3), 1.53 (br s, 2H, N*H*), 2.39 (ttt, $^3J_{HH}$ = 9.2, 3.7 Hz, 1H, C*H*), 2.71 (dd, $^2J_{HH}$ = 10.5 Hz, $^3J_{HH}$ = 9.2 Hz, 2H, CH_2), 3.45 (dt, $^2J_{HH}$ = 10.5 Hz, $^3J_{HH}$ = 3.7 Hz, 2H, CH_2). ^{13}C{^{1}H} NMR (toluene-d_8) δ: 28.1 (vt, ^vJ = 3.2 Hz, *C*H_3), 28.5 (vt, ^vJ = 3.8 Hz, *C*H_3), 38.0 (vt, ^vJ = 7.2 Hz, *C*Me$_3$), 38.1 (vt, ^vJ = 10.6 Hz, *C*Me$_3$), 58.3 (vt, ^vJ = 8.4 Hz, *C*H_2), 80.2 (t, $^2J_{CP}$ = 1.8 Hz, *C*H). ^{31}P{^{1}H} NMR (C_6D_6), δ: 130.9 (s).

Computational Details. The calculations were done with Gaussian 98 (revision A.11).[26] All geometries were first optimized using the ONIOM(*m*PW1PW91:bs1/HF:LANL2MB) approach,[27,28] and the nature of the stationary points was verified by frequency calculations which were used to calculate ZPE without scaling. In the ONIOM calculations, all *tert*-butyl groups were included in the "low" level, while the rest of the atoms were assigned to the "high" level. Subsequently, all geometries were fully optimized without symmetry or internal coordinate constraints at the *m*PW1PW91/bs2 level using the atomic coordinates and force constants provided by the ONIOM calculations. The basis sets bs1 included LANL2DZ (associated with the ECPs for Ru, P, and Cl atoms) augmented by a single *p* polarization function for the hydride and *d* polarization functions for all C, N, P, and Cl atoms.[29] The basis set bs2 included SDD + ECP for Ru, 6-31G for the CH_3 groups, 6-31G(p) for the hydride, and 6-31G(d) for all other atoms.[28] The Synchronous Transit-Guided Quasi-Newton (STQN) method QST3[30] was used to optimize transition states **TS1**−**TS4**. Motions corresponding to the single imaginary frequencies were visually checked. Unless mentioned otherwise, all reported energies are Gibbs free energies at 298 K.

Acknowledgment. We gratefully acknowledge the Natural Sciences and Engineering Research Council of Canada (NSERC) and the Ontario Government for funding.

Supporting Information Available: Complete ref 26, CIF files for complexes **2a**, **3c**, and **4**. This material is available free of charge via the Internet at http://pubs.acs.org.

JA065249G

(26) Frisch, M. J. et al. *Gaussian 98*, revision A.11; Gaussian, Inc.: Pittsburgh, PA, 2001.
(27) (a) Adamo, C.; Barone V. *J. Chem. Phys.* **1998**, *108*, 664. (b) Perdew, J. P.; Burke, K.; Wang, Y. *Phys. Rev. B* **1996**, *54*, 16533. (c) Burke K.; Perdew, J. P.; Wang, Y. In *Electronic Density Functional Theory: Recent Progress and New Directions*; Dobson, J. F., Vignale, G., Das, M. P., Eds.; Plenum: 1998.
(28) (a) Svensson, M.; Humbel, S.; Froese, R. D. J.; Matsubara, T.; Sieber, S.; Morokuma, K. *J. Phys. Chem.* **1996**, *100*, 19357. (b) Maseras, F. *Chem. Commun.* **2000**, 1821.
(29) For more information about basis sets implemented in Gaussian and references, see: Frish, A.; Frish, M. J.; Trucks, G. W. *Gaussian 03 User's Reference*; Gaussian, Inc.: Pittsburgh, PA, 2003. The basis sets are also available from the Extensible Computational Chemistry Environment Basis Set Database, which is developed and distributed by the Molecular Science Computing Facility, Environmental and Molecular Sciences Laboratory, which is part of the Pacific Northwest Laboratory, P.O. Box 999, Richland, WA 99352, USA (www.emsl.pnl.gov/forms/basisform.html).
(30) Peng, C.; Ayala, P. Y.; Schlegel, H. B.; Frisch, M. J. *J. Comput. Chem.* **1996**, *17*, 49.